

DMD #50583

**Quantitative prediction of repaglinide-rifampicin complex drug interactions using dynamic and static mechanistic models: Delineating differential CYP3A4 induction and OATP1B1 inhibition potential of rifampicin**

Manthena V. S. Varma, Jian Lin, Yi-An Bi, Charles J. Rotter, Odette A. Fahmi, Justine L. Lam, Ayman F. El-Kattan, Theunis C. Goosen and Yurong Lai

Pharmacokinetics Dynamics and Metabolism, Pfizer Global Research and Development, Pfizer Inc., Groton, Connecticut (M.V.V., J.L., Y.B., C.J.R., O.A.F., A.F.E., T.C.G, Y.L), and La Jolla, California (J.L.L.)

DMD #50583

**Running title:** Prediction of repaglinide-rifampicin DDIs

**Corresponding Author:**

Manthena V. S. Varma, Ph.D.

Department of Pharmacokinetics, Dynamics, and Metabolism, MS 8220-2451, Pfizer World

Wide Research and Development, Pfizer Inc., Groton, CT 06340; Phone:+1-860-715-0257. Fax:

+1-860-441-6402. E-mail: manthena.v.varma@pfizer.com.

Number of text pages:	33
Number of tables:	2
Number of Figures:	5
Number of references:	61
Number of words in Abstract:	243
Number of words in Introduction:	735
Number of words in Discussion:	1707

## ABSTRACT

Repaglinide is mainly metabolized by cytochrome-P-450 (CYP)2C8 and CYP3A4, and is also a substrate to hepatic uptake transporter, organic anion transporting polypeptide (OATP)1B1. The purpose of this study is to predict the “dosing-time” dependent pharmacokinetic interactions of repaglinide with rifampicin, using mechanistic models. *In vitro* hepatic transport of repaglinide, characterized using sandwich-cultured human hepatocytes, and intrinsic metabolic parameters were used to build a dynamic whole-body physiologically-based pharmacokinetic (PBPK) model. The PBPK model adequately described repaglinide plasma concentration-time profiles; and successfully predicted area under the plasma concentration-time curve ratios of repaglinide (within  $\pm 25\%$  error), dosed (staggered 0-24h) after rifampicin treatment, when primarily considering induction of CYP3A4 and reversible inhibition of OATP1B1 by rifampicin. Further, a static mechanistic “extended net-effect” model incorporating transport and metabolic disposition parameters of repaglinide and interaction potency of rifampicin was devised. Predictions based on the static model are similar to that observed in the clinic (average error  $\sim 19\%$ ), as well as similar to the PBPK model predictions. Both the models suggested that the combined effect of increased gut extraction and decreased hepatic uptake caused minimal repaglinide systemic exposure change when repaglinide is dosed simultaneously or 1h after the rifampicin dose. On the other hand, isolated induction effect as a result of temporal separation of the two drugs translated to  $\sim 5$ -fold reduction in repaglinide systemic exposure. In conclusion, both dynamic and static mechanistic models are instrumental in delineating the quantitative contribution of transport and metabolism in the dosing-time dependent repaglinide-rifampicin interactions.

## INTRODUCTION

Drug-drug interactions (DDIs) associated with membrane transporters and metabolizing enzymes can lead to severe adverse reactions and/or a reduced pharmacological effects. *In vitro* tools are valuable in assessing the involvement of such individual processes in the drug disposition. For example, human liver microsomes are extensively used in predicting the metabolic clearance of xenobiotics in human (Obach et al., 2006). Recently, sandwich-cultured human hepatocytes (SCHH) were demonstrated as an useful *in vitro* tool to characterize the hepatobiliary transport (Abe et al., 2009; Jones et al., 2012; Kimoto et al., 2012). However, integrating these *in vitro* data to quantitatively project the interplay between metabolizing enzymes and transporters and their impact on drug disposition continues to be a challenge. Recently physiologically based pharmacokinetic (PBPK) modeling has demonstrated utility in predicting drug pharmacokinetics and evaluating the DDI potential (Huang and Rowland, 2012; Rostami-Hodjegan, 2012). The implementation of PBPK is being increasingly considered in drug discovery and development, due to its versatility and the availability of commercial packages (e.g. Gastroplus, PK-Sim, Simcyp, etc.). Furthermore, the latest US Food and Drug Administration (USFDA) and European Medicines Agency (EMA) guidelines on drug interactions suggested the use of mechanistic modeling to quantitatively predict the magnitude of DDIs in various clinical situations (EMA, 2012; USFDA, 2012).

Repaglinide is an antidiabetic drug, used to treat type 2 or non-insulin dependent diabetes mellitus (Scott, 2012). It lowers the blood glucose levels by stimulating the release of insulin from pancreas while interfering with the ATP-dependent potassium channels in the  $\beta$ -cell membrane. Repaglinide is majorly metabolized by the cytochrome P450 (CYP) isoenzymes,

CYP2C8 and CYP3A4, and it is also a substrate to hepatic uptake transporter, organic anion transporter polypeptide (OATP)1B1 (Bidstrup et al., 2003; Niemi et al., 2003c; Kajosaari et al., 2005a; Niemi et al., 2005; Menochet et al., 2012; Sall et al., 2012). The plasma exposure of repaglinide is altered by several drugs that inhibit CYP2C8, CYP3A4 and/or OATP1B1 (Tornio et al., 2012). Notably, gemfibrozil caused an increase in area under the plasma concentration-time curve (AUC) of repaglinide up to 8.3-fold (Honkalammi et al., 2011a), mainly due to mechanism-based inactivation of CYP2C8 by its major circulating metabolite, gemfibrozil 1-*O*- $\beta$ -glucuronide, and competitive inhibition of OATP1B1 by both gemfibrozil and the metabolite (Fujino et al., 2003; Shitara et al., 2004). Oxidative biotransformation of repaglinide by both CYP2C8 and CYP3A4, with CYP3A4 fraction metabolism ( $fm$ )<sub>CYP3A4</sub> of 0.29-0.45, has been reported *in vitro* (Bidstrup et al., 2003; Kajosaari et al., 2005a). However, an apparent *in vitro*-*in vivo* disconnect in  $fm$  of the two CYPs has been suggested, based on the recent clinical repaglinide-gemfibrozil DDIs studies (Honkalammi et al., 2011a; Honkalammi et al., 2012). In these studies, using a static modeling approach, repaglinide  $fm$ <sub>CYP2C8</sub> was estimated to be >0.85 *in vivo*. Previously, we developed a whole-body PBPK model for repaglinide, which suggested that repaglinide systemic disposition is dependent on the hepatic uptake clearance, and that the change in its AUC is influenced by hepatic uptake clearance, intrinsic metabolic clearances and the  $fm$  (Varma et al., 2013). Our mechanistic evaluation demonstrated that repaglinide-gemfibrozil DDIs can be quantitatively described with the *in vitro*  $fm$  values.

The anti-tuberculosis agent, rifampicin, is a typical inducer of drug transporters and metabolizing enzymes, particularly CYP3A4 (Niemi et al., 2003a). DDIs were reported when repaglinide was administered with rifampicin. Notably, there is a significant impact of repaglinide “dosing-time”

relative to rifampicin treatment on the magnitude of repaglinide systemic exposure change. For example, only a 31% decrease in repaglinide AUC was observed, when repaglinide was ingested 1h after the last dose of rifampicin treatment (Hatorp et al., 2003). In a separate study, repaglinide AUC decreased 57% when administered 12.5h following the last oral dose of rifampicin (Niemi et al., 2000). Yet in another study, repaglinide AUC was decreased by ~50% and 80% when administered concomitantly and 24h after the last rifampicin dose, respectively (Bidstrup et al., 2004). We hypothesized that the effects of rifampicin on the repaglinide disposition could be complex – involving induction of CYP3A4 and inhibition of hepatic uptake and/or metabolism; and these multiple mechanisms need to be considered to quantitatively rationalize the observed dosing-time dependent interactions. In this study, we utilized a dynamic mechanistic (whole-body PBPK) model of repaglinide to simulate the plasma concentration-time profiles, and further assess the repaglinide dosing-time dependent interactions with rifampicin. In addition, a static mechanistic “extended net-effect” model considering enzyme- and transporter-mediated disposition of repaglinide was developed to assess the interactions with rifampicin.

## MATERIALS AND METHODS

### PBPK Modeling and Simulations

Whole-body PBPK modeling and simulations of clinical pharmacokinetics and DDIs were performed using population-based ADME simulator, Simcyp (version 11.0, SimCYP Ltd, Sheffield, UK). Repaglinide model was build using the physicochemical properties, *in vitro* preclinical data such as human plasma unbound fraction ( $f_u$ ), blood-to-plasma ratio ( $R_b$ ), metabolic intrinsic clearance values, etc. (Table 1). Complete details of the repaglinide PBPK model have been described elsewhere (Varma et al., 2013). In brief, full-PBPK model using Rodgers et al. method (Rodgers and Rowland, 2006) considering rapid equilibrium between blood and tissues was adopted to obtain the distribution of repaglinide into all organs, except liver. Permeability-limiting hepatic disposition of repaglinide was considered, for which, sinusoidal active uptake intrinsic clearance and passive diffusion obtained from SCHH studies were incorporated (Varma et al., 2013). Hepatic microsomal  $CL_{int,met}$  and fraction metabolism contribution of CYP3A4 to the total metabolic clearance ( $f_{m_{CYP3A4}}$ ) used in the current modeling represent 131  $\mu\text{l}/\text{min}/\text{mg}$ ) and 0.29, respectively (Kajosaari et al., 2005a; Varma et al., 2013). The model with these initial (transport and metabolism) input parameters resulted in underprediction of hepatic clearance. Therefore, an empirical scaling factor for the hepatic sinusoidal active uptake ( $SF_{active} = 16.9$ ), estimated by ‘top-down’ model fitting to the intravenous data was applied, while keeping the rest of the input parameters same as that of the initial model (Watanabe et al., 2009; Jones et al., 2012; Varma et al., 2012b). Advanced dissolution, absorption and metabolism (ADAM) model was adopted to capture intestinal absorption and predict oral pharmacokinetics of repaglinide. Rifampicin model (input

parameters, Table 1) was directly adopted from Simcyp compound library (Varma et al., 2012b). Rifampicin interaction parameters against CYP3A4, CYP2C8 and OATP1B1 were generated in-house or extracted from literature. Each simulation was performed for 50 subjects (5 trials  $\times$  10 subjects). The virtual populations of healthy subjects had a body weight of 70 kg, with age ranging from 18 to 65 years, and included both sexes. Dose, dosing interval, and dosing duration of repaglinide and rifampicin were identical to that reported in individual clinical studies.

### Static mechanistic “extended net-effect” model

The area under the plasma concentration-time curve ratio (AUCR) of repaglinide in the presence ( $AUC'_{po}$ ) and absence ( $AUC_{po}$ ) of rifampicin treatment can be described as in Eq. 1 (Fahmi et al., 2008).

$$AUCR = \frac{AUC'_{po}}{AUC_{po}} = \frac{Fa' \cdot Fg'}{Fa \cdot Fg} \cdot \frac{CL_{int,h}}{CL'_{int,h}} \quad (1)$$

Fa' and Fa represent the fraction of drug absorbed from the intestine; and Fg' and Fg represent the fraction of drug escaping gut-wall metabolism in the presence and the absence of rifampicin, respectively. Repaglinide is a highly permeable drug with almost complete absorption (>95%) (Hatorp et al., 1998; Varma et al., 2010), and therefore the Fa'/Fa term was assumed to be 1 (see Discussion).  $CL_{int,h}$  and  $CL'_{int,h}$  represent the intrinsic hepatic clearance in the absence and presence of the rifampicin, respectively. Due to the primary involvement of active uptake and CYP-mediated metabolism in the hepatic disposition of repaglinide (Varma et al., 2013), its overall intrinsic hepatic clearance can be mathematically defined by extended clearance concept, as in Eq. 2 (Liu and Pang, 2005; Shitara et al., 2006; Shitara and Sugiyama, 2006; Camenisch and Umehara, 2012; Barton et al., 2013).



$$CL_{int,h} = PS_{uptake} \cdot \frac{(CL_{int,CYP3A4} + CL_{int,CYP2C8})}{(PS_{efflux} + CL_{int,CYP3A4} + CL_{int,CYP2C8})} \quad (2)$$

$$PS_{uptake} = (SF_{active} \cdot PS_{influx,active} + PS_{pd})$$

$$PS_{efflux} = (PS_{efflux,active} + PS_{pd})$$

where  $PS_{uptake}$  and  $PS_{efflux}$  are the uptake and efflux intrinsic clearances across the sinusoidal membrane.  $PS_{influx,active}$ ,  $PS_{efflux,active}$  and  $PS_{pd}$  are sinusoidal active uptake, active efflux and passive diffusion intrinsic clearances, respectively.  $CL_{int,CYP3A4}$  and  $CL_{int,CYP2C8}$  are metabolic intrinsic clearances.

Assuming active efflux across sinusoidal membrane ( $PS_{efflux,active}$ ) is negligible, Eq. 2 can be rewritten as:

$$CL_{int,h} = (SF_{active} \cdot PS_{influx,active} + PS_{pd}) \cdot \frac{(CL_{int,CYP3A4} + CL_{int,CYP2C8})}{(PS_{pd} + CL_{int,CYP3A4} + CL_{int,CYP2C8})} \quad (3)$$

Similar to that used in the PBPK model,  $SF_{active}$  represents empirical scaling factor for active uptake estimated by matching the *in vitro*  $CL_{int,h}$  to the *in vivo*  $CL_{int,h}$  obtained from intravenous pharmacokinetics of repaglinide (Eq. 9) (Table 1). The *in vitro* intrinsic values were scaled assuming the following:  $118 \times 10^6$  hepatocytes  $g^{-1}$  liver, 39.8 mg microsomal protein  $g^{-1}$  liver, 24.5 g liver  $kg^{-1}$  body weight (mean values used in healthy volunteers population file of Simcyp V11).

In the presence of rifampicin, the expected net effect of competitive inhibition of CYP3A4 and CYP2C8, induction of CYP3A4 and competitive inhibition of active uptake (OATP1B1) can be illustrated by Eq. 4.

$$CL'_{int,h} = \left( \frac{SF_{active} \cdot PS_{influx,active}}{RI_h} + PS_{pd} \right) \cdot \frac{\left( \frac{CL_{int,CYP3A4}}{RI_h \cdot IND_h} + \frac{CL_{int,CYP2C8}}{RI_h} \right)}{\left( PS_{pd} + \frac{CL_{int,CYP3A4}}{RI_h \cdot IND_h} + \frac{CL_{int,CYP2C8}}{RI_h} \right)} \quad (4)$$

$RI_h$  is the competitive inhibition term, and  $IND_h$  is the hepatic CYP3A4 induction term (Eqs. 5) (Fahmi et al., 2008; Giacomini et al., 2010; Barton et al., 2013).

$$RI_h = 1 + \frac{[I_{u,max,in}]}{Ki}$$

$$IND_h = \frac{1}{\left( 1 + \frac{E_{max} \cdot [I_{u,max,in}]}{[I_{u,max,in}] + EC_{50}} \right)} \quad (5)$$

$Ki$  is the inhibition constant and  $I_{u,max,in}$  is the maximum unbound rifampicin concentration at the inlet to liver after repaglinide dosing. Rifampicin fraction unbound in the *in vitro* incubations was assumed to be one. The values were taken from portal vein concentration-time profile predicted using PBPK (Simcyp) model (Varma et al., 2012b).  $E_{max}$  represent the maximum fold induction, and  $EC_{50}$  is the concentration of inducer associated with half-maximum induction.

Assuming the gut metabolism of repaglinide is determined by only CYP3A4 (CYP2C8 expression in the gut is negligible) (Paine et al., 2006), the change of the fraction of drug escaping intestinal extraction in the presence of perpetrator can be defined by Eq. 6 (Fahmi et al., 2008).

DMD #50583

$$\frac{Fg'}{Fg} = \frac{1}{\frac{(1 - Fg)}{RI_g \cdot IND_g} + Fg} \quad (6)$$

$RI_g$ , and  $IND_g$  are the reversible inhibition and induction terms for CYP3A4-mediated gut metabolism Eqs. 7.

$$RI_g = 1 + \frac{[I_{u,gut}]}{Ki}$$
$$IND_g = \frac{1}{\left(1 + \frac{E_{max} \cdot [I_{u,gut}]}{[I_{u,gut}] + EC_{50}}\right)} \quad (7)$$

$I_{u,gut}$ , the free intestinal rifampicin concentration, was estimated by Eq. 8.

$$[I_{u,gut}] = \frac{Dose \cdot Ka \cdot fa \cdot f_{u,gut}}{Q_{gut}} \quad (8)$$

Dose,  $Ka$ ,  $fa$ ,  $f_{u,gut}$  and  $Q_{gut}$  (248 mL/min (Fahmi et al., 2008)) represent total dose given orally, absorption rate constant, fraction absorbed, fraction unbound in the gut and enterocytic blood flow, respectively.  $Fg$  of repaglinide was estimated to be 0.94 based on the current PBPK (Simcyp) model. Also, to maintain consistency between the model predictions, all the parameters used for static modeling are the same as used for PBPK modeling (Table 1).

*In vivo*  $CL_{int,h}$  was calculated using the well-stirred liver model (Pang and Rowland, 1977).

$$CL_{int,h} = \frac{CL_h}{f_{u,b} \cdot \left(1 - \frac{CL_h}{Q_h}\right)} \quad (9)$$

$CL_h$  is the hepatic blood clearance obtained from intravenous total plasma clearance corrected for  $R_b$ . The  $f_{u,b}$  represents the fraction unbound in blood and  $Q_h$  represents the average hepatic blood flow of 20.7 mL/min/kg (Kato et al., 2003).

### Model Predictability

The model predicted AUC ratios were compared to the observed values using percentage prediction error (PPE) Eq. 10. Prediction bias and precision were also assessed with root mean square error (RMSE) Eq. 11 and average fold error (AFE) Eq. 12.

$$PPE (\%) = 100 \cdot \frac{1}{N} \sum \frac{|\text{Predicted} - \text{Observed}|}{\text{Observed}} \quad (10)$$

$$RMSE = \sqrt{\frac{\sum (\text{Predicted} - \text{Observed})^2}{N}} \quad (11)$$

$$AFE = 10^{\frac{1}{N} \sum \left| \log_{10} \frac{\text{Predicted}}{\text{Observed}} \right|} \quad (12)$$

$N$  is the number of observations.

## RESULTS

### Dynamic (PBPK) model predictions

A whole-body PBPK model, assuming permeability-limited hepatic disposition, was used to assess repaglinide DDIs with rifampicin. The PBPK model adequately described repaglinide plasma concentration-time profile after a single intravenous and an oral dose (Figure 1A). The simulated mean plasma concentration-time profile of repaglinide following rifampicin treatment is in good agreement with the observed data, where repaglinide was dosed 12.5h after the last dose of rifampicin (Figure 1B). Furthermore, the magnitude of repaglinide-rifampicin interactions with concomitant or time-separated dosing are well predicted; wherein, the model predicted least and largest changes in exposure when repaglinide was administered 1h and 24h after the last dose of rifampicin, respectively (Figure 2). For all the DDI predictions, rifampicin was considered to induce CYP3A4 activity ( $EC_{50} = 0.228\mu\text{M}$ ;  $E_{\text{max}} = 49.2$ ), as well as reversibly inhibit OATP1B1 ( $K_i = 0.93\mu\text{M}$ ), CYP3A4 ( $K_i = 18.5\mu\text{M}$ ) and CYP2C8 ( $K_i = 30.2\mu\text{M}$ ) (Table 1).

### Static mechanistic model predictions

A static mechanistic model was devised based on the extended clearance concept (Shitara et al., 2006) to predict the change in overall hepatic clearance. The predictions based on static model are in good agreement with the observed values, as well as with the AUCRs predicted by the PBPK model (Figure 2). In general, the static model predicted AUCR within 25% of the observed values (Table 2). Interestingly, sensitivity analysis of  $f_{\text{mCYP3A4}}$  input with a fixed  $CL_{\text{int,met}}$  ( $131\mu\text{l}/\text{min}/\text{mg}$ ) showed no significant effect on the AUCRs (Figure 3).

### **Individual components of the interaction**

Figure 4 shows the predicted changes in the individual components of CYP3A4 induction, OATP1B1 inhibition and CYPs inhibition, and the net effect of rifampicin on repaglinide pharmacokinetics. Both the dynamic and static models suggested that only OATP1B1 inhibition leads to increase in repaglinide plasma exposure by ~2-3 fold, whereas the CYP3A4 induction effect resulted in AUCR of ~0.2-0.3 fold. Models predict that rifampicin show competitive inhibitory effect on OATP1B1 upto ~12h postdose resulting in partial masking of CYP3A4 induction effect when both drugs are administered in temporal proximity. In contrary, rifampicin has a negligible inhibitory effect on CYPs-mediated metabolism, even with concomitant dosing. In general, the CYP3A4 induction and OATP1B1 inhibition effects of rifampicin predicted by static mechanistic model are larger than that noted with dynamic model, presumably due to the use of maximum inlet concentration. Nevertheless, net-effect of the multiple interaction components resulted in prediction of DDIs similar to that observed in the clinic.

Based on PBPK modeling, rifampicin treatment resulted in a gradual increase in CYP3A4 activity in the intestine and liver by ~25-fold and ~15-fold, respectively (Figure 5A). The induction effect of rifampicin was higher at intestine, presumably due to higher exposure at the gut. Following rifampicin treatment, fraction extracted in the gut increased from ~6% of the dose to ~55%, implicating that the major site of repaglinide elimination shifts from liver in the control group to gut in rifampicin treatment group (Figure 5B). Interestingly, increased CYP3A4 activity in liver has a minimal effect on the hepatic clearance of repaglinide. For example,  $CL_{int,h}$  was reduced by only ~27%, while  $F_g$  was reduced by ~74% compared to the control, when repaglinide was dosed 24h after rifampicin treatment (Table 2). On the other hand, rifampicin

DMD #50583

showed upto a maximum of ~60% OATP1B1 inhibition and showed no accumulation following multiple rifampicin once-daily doses (Figure 5C). Finally, the dynamic modeling suggested that the induction effect returned to the baseline only after 4 days following the last dose of 7-day rifampicin treatment (Figure 5A).

## DISCUSSION

This mechanistic evaluation demonstrated that differential effects of rifampicin on CYP3A4 and OATP1B1 causes varied degree of change in repaglinide systemic exposure – depending on the temporal separation of administration of two drugs. The pharmacokinetics of repaglinide was highly affected when repaglinide was administered 24h after the last dose of rifampicin pretreatment (Bidstrup et al., 2004). However, repaglinide ingested concomitantly or 1h after the last dose of rifampicin showed only low to moderate reduction in repaglinide systemic exposure (AUCR ~0.52-0.68) (Hatorp et al., 2003; Bidstrup et al., 2004). Clearly, these different clinical observations can be accurately predicted using the PBPK model and the proposed static mechanistic (extended net-effect) model.

The systemic clearance of repaglinide estimated using *in vitro* enzyme kinetics considerably underpredicted *in vivo* clearance, suggesting a key role of hepatic uptake in its disposition (Hatorp et al., 1998; Kajosaari et al., 2005a). Our previous *in vitro* transport studies and mechanistic modeling indicated that the systemic clearance of repaglinide is determined mainly by the hepatic uptake process (Varma et al., 2013). Here, we developed PBPK and static mechanistic models for repaglinide incorporating the hepatic transport- and enzyme-mediated disposition processes, based on the *in vitro* input parameters. Both the models directly using the *in vitro* transport parameters, however, underpredicted repaglinide systemic clearance, presumably due to discrepancy in the *in vitro-in vivo* extrapolation of transporter-mediated uptake activity. There are many possible reasons for the potential *in vitro-in vivo* discrepancy in the hepatic transporter activity, including down-regulation of transporter protein and/or partial loss of functional activity in the *in vitro* system (Jones et al., 2012; Varma et al., 2012b; Varma



et al., 2013). Therefore, an empirical scaling factor for  $PS_{\text{active}}$ , estimated based on “top-down” fitting to human intravenous plasma concentration-time profiles, was incorporated in the PBPK model (Figure 1) (Jones et al., 2012; Varma et al., 2012b; Varma et al., 2013). Similarly, scaling factor for active uptake was applied to the static mechanistic model to match the *in vitro* hepatic clearance to that observed *in vivo*. The scaling factors estimated for both the models were comparable (Table 1). Overall, the whole-body PBPK and the static mechanistic models, assuming permeability-limited hepatic disposition, adequately described the pharmacokinetics of repaglinide.

Rifampicin is a potent inducer of CYPs, and also shows *in vitro* inhibition of CYP3A4 and CYP2C8. The net effect of significant inductive as well as inhibitory effects of rifampicin on CYP-mediated metabolism was thought to be responsible for the observed dosing-time dependent repaglinide-rifampicin DDIs (Niemi et al., 2000; Bidstrup et al., 2004). However, the current assessment using *in vitro*  $K_i$  of CYP3A4 (18.5 $\mu$ M) and CYP2C8 (30.2 $\mu$ M) demonstrated that the acute inhibition of metabolism had only a minimal role (Figure 4). In contrary, reduction in hepatic uptake via inhibition of OATP1B1 caused increase in AUC, which when combined with the induction potential of rifampicin yielded a good prediction of AUCRs. Interestingly, change in the overall hepatic intrinsic clearance due to only CYP3A4 induction following rifampicin treatment was minimal compared to the reduction noted with  $F_g$  (Table 2). Presumably, hepatic uptake being the rate-determining step in the systemic clearance of repaglinide, change in only metabolic activity (induction or inhibition) do not significantly alter the overall hepatic clearance (Maeda et al., 2011; Varma et al., 2013). Moreover, sensitivity analysis suggested no significant effect of  $f_{m_{\text{CYP3A4}}}$  on the predicted AUCR (Figure 3).

Collectively, the mechanistic modeling suggests that the net-effect of increased CYP3A4 activity (mainly in gut) and decreased hepatic uptake determine the magnitude of repaglinide-rifampicin interactions.

Additional rifampicin-mediated induction of efflux transporters, such as P-glycoprotein (P-gp), might also play a role in decreasing the repaglinide exposure (Westphal et al., 2000). Furthermore, differential acute inhibition of intestinal efflux and chronic induction of CYPs and/or P-gp, by rifampicin, could explain dosing-time dependent differences in repaglinide exposure. Rifampicin is a moderate P-gp inhibitor ( $IC_{50} = 169\mu M$ ) *in vitro* (Reitman et al., 2011). Also, oral exposure of digoxin was shown to increase by rifampicin co-dosing, presumably due to intestinal P-gp inhibition (Reitman et al., 2011). Based on our assessment, repaglinide is a biopharmaceutics class I drug (Wu and Benet, 2005; Varma et al., 2012a): high permeability (Caco-2 permeability  $\sim 26 \times 10^{-6}$  cm/s), moderate solubility (68 $\mu$ g/mL) (Mandic and Gabelica, 2006), low dose (<4mg) and complete absorption (>95%). Thus, while repaglinide has been shown to be a P-gp substrate with high asymmetric transport across MDCK-MDR1 cells (Korzekwa et al., 2012), P-gp is expected to have a limited role in determining the extent of repaglinide absorption (Varma et al., 2005). On the other hand, the full inductive effect is believed to be attained in about 7 days after once-daily rifampicin treatment (Niemi et al., 2003a). The PBPK model simulation of CYP3A4 activity is consistent with this, and further suggests that the average metabolic activity starts declining after 24h of the last dose of rifampicin (Figure 5A). Therefore, it is unlikely that the dosing-time dependent interactions observed (low when concomitant dosing versus high interaction when dosed 24h after rifampicin) are due to further enhanced induction.

Although to a lesser extent relative to CYP3A4 induction, rifampicin also induces CYP2C8 – which plays a key role in repaglinide elimination (Niemi et al., 2003a). It is unclear from the existing data, if which and to what extent of the hepatic CYP isoenzymes were induced by rifampicin. However, such information can be derived if the plasma profiles of repaglinide circulating metabolites are available. Formation of metabolites M1 and M4 is dependent on the CYP3A4 and CYP2C8, respectively (Sall et al., 2012). Gemfibrozil, a potent mechanism-based inactivator of CYP2C8, drastically decreased plasma circulating M4 levels, while significantly increasing M1 concentrations (Kajosaari et al., 2005b; Tornio et al., 2008; Honkalammi et al., 2011b; Honkalammi et al., 2011a; Honkalammi et al., 2012). Similar differential metabolite pharmacokinetics may delineate the CYP3A4 versus CYP2C8 role in the observed induction effect. Nevertheless, we postulate that CYP2C8 induction only has a minimal effect on repaglinide pharmacokinetics, because (i) repaglinide systemic clearance is majorly determined by the hepatic uptake clearance and an increase in hepatic metabolic activity is less likely to affect the systemic clearance (Table 2), and (ii) as noted with the simulations here, increase in the gut metabolism is the major driver for observed decrease in repaglinide exposure (particularly, when rifampicin and repaglinide doses were separated by >12h), and CYP2C8 contribution to the gut metabolism is believed to be relatively low (Paine et al., 2006). Nevertheless, although no clinical evidences exist, expression and *in vitro* data suggests that rifampicin significantly induce the intestinal CYP2C8 and CYP2C9 isoforms and may partially contribute to such interactions (Lapple et al., 2003; Glaeser et al., 2005).

Repaglinide lowers blood glucose levels by stimulating the release of insulin from the pancreas while interfering with the ATP-dependent potassium channels in the  $\beta$ -cell membrane. Clinical

DDI studies often demonstrated relationship between plasma exposure and pharmacodynamic activity of repaglinide, with increased glucose lowering activity by cyclosporine and gemfibrozil and decreased activity following rifampicin treatment (Niemi et al., 2003b; Honkalammi et al., 2012; Tornio et al., 2012). Therefore, an increase in repaglinide dose based on clinical response to therapy should be considered when it is coadministered with strong CYP inducers such as rifampicin and other therapeutic agents such as carbamazepine, phenytoin, efavirenz, St. John's wort, etc (Luo et al., 2002; Niemi et al., 2003a). Unlike rifampicin, many of these CYP inducers do not inhibit OATPs at the clinically relevant concentrations and therefore the interactions are expected to be independent of dosing-time in relative to repaglinide dose.

Involvement of similar dual effects of rifampicin has been hypothesized to explain DDIs with other CYPs substrates. For example, a single intravenous dose of the rifampicin increased the AUC of glyburide by ~120%, presumably due to acute inhibition of hepatic uptake (Zheng et al., 2009). However, glyburide AUC reduced when concomitantly dosed with rifampicin following a chronic oral treatment; and a further reduction in AUC was noted when glyburide was dosed two days after the last dose of rifampicin. Atorvastatin-rifampicin interactions serve as another example, wherein a single intravenous dose of rifampicin increased atorvastatin AUC by ~7-fold (Lau et al., 2007), while atorvastatin dosed 17h after a 5-day oral rifampicin treatment led to significant decrease in its systemic exposure (Backman et al., 2005). In a microdosing study, atorvastatin AUC was shown to be markedly affected by a single rifampicin dose administered simultaneously, but not by an intravenous dose of itraconazole, a potent CYP3A4 inhibitor, suggesting that the hepatic uptake is the rate-determining process in the hepatic clearance of atorvastatin (Maeda et al., 2011). Therefore, as demonstrated in the current study, the marked

reduction in atorvastatin AUC by chronic rifampicin treatment noted in the clinic (Backman et al., 2005) could be explained by the CYP3A4 induction at the gut, with a minimal contribution of increased hepatic metabolic activity. As shown in the current study, similar dynamic and static mechanistic modeling utilizing *in vitro* transport and metabolic kinetics can be useful in delineating the quantitative function of individual components of these interactions.

For OATPs substrate drugs like repaglinide, where systemic clearance is determined by the hepatic uptake as well as metabolism, mechanistic considerations assuming permeability-limited disposition are needed to accurately predict complex DDIs (Varma et al., 2013). As demonstrated in this study, the mechanistic modeling approaches using both the dynamic and static models are useful for assessing the DDI potential. Notably, when the input parameters remain the same, both models yielded similar results. The proposed static model has the advantage of being simple and more transparent and can be valuable for quantitative predictions of DDI scenarios in the drug development. Nevertheless, dynamic models can help consider extremes in population variability by incorporating variability in the *in vivo* drug disposition and polymorphic clearance pathways or by simulating drug disposition in disease states or special populations (Rowland et al., 2011).

In conclusion, the current PBPK and static mechanistic model-based analysis suggest that the dual effects of CYP3A4 induction and competitive inhibition of OATP1B1-mediated hepatic uptake are apparent when both drugs are administered in temporal proximity, whereas the CYP3A4 induction effect can be isolated if repaglinide and rifampicin doses are sufficiently separated in time (>12h after rifampicin dose). Finally, since hepatic disposition is uptake rate-

DMD #50583

limiting, increased CYP3A4 activity in the gut, but not liver, majorly contributes to the increased metabolic clearance of repaglinide following rifampicin treatment.

DMD #50583

### **Authorship contributions**

*Participated in research design:* M.V.S.V., Y.L.

*Contributed new reagents or analytic tools:* M.V.S.V.

*Conducted experiments:* M.V.S.V., J.L., Y.B., C.J.R.

*Performed data analysis:* M.V.S.V., O.A.F., J.L., J.L.L., A.F.E., T.C.G, Y.L

*Wrote or contributed to the writing of the manuscript:* M.V.S.V., J.L., Y.B., C.J.R., O.A.F.,  
J.L.L., A.F.E., T.C.G, Y.L.

## REFERENCES

- Abe K, Bridges AS, and Brouwer KL (2009) Use of sandwich-cultured human hepatocytes to predict biliary clearance of angiotensin II receptor blockers and HMG-CoA reductase inhibitors. *Drug Metab Dispos* **37**:447-452.
- Backman JT, Luurila H, Neuvonen M, and Neuvonen PJ (2005) Rifampin markedly decreases and gemfibrozil increases the plasma concentrations of atorvastatin and its metabolites. *Clin Pharmacol Ther* **78**:154-167.
- Barton HA, Lai Y, Goosen TC, Jones HM, El-Kattan AF, Gosset JR, Lin J, and Varma MV (2013) Model-based approaches to predict drug-drug interactions associated with hepatic uptake transporters: preclinical, clinical and beyond. *Expert Opin Drug Metab Toxicol*:(in press).
- Bidstrup TB, Bjornsdottir I, Sidemann UG, Thomsen MS, and Hansen KT (2003) CYP2C8 and CYP3A4 are the principal enzymes involved in the human in vitro biotransformation of the insulin secretagogue repaglinide. *Br J Clin Pharmacol* **56**:305-314.
- Bidstrup TB, Stilling N, Damkier P, Scharling B, Thomsen MS, and Broesen K (2004) Rifampicin seems to act as both an inducer and an inhibitor of the metabolism of repaglinide. *Eur J Clin Pharmacol* **60**:109-114.
- Camenisch G and Umehara K (2012) Predicting human hepatic clearance from in vitro drug metabolism and transport data: a scientific and pharmaceutical perspective for assessing drug-drug interactions. *Biopharm Drug Dispos* **33**:179-194.
- EMA (2012) Guideline on the Investigation of Drug Interactions. *Committee for Human Medicinal Products (CHMP)*.
- Fahmi OA, Maurer TS, Kish M, Cardenas E, Boldt S, and Nettleton D (2008) A combined model for predicting CYP3A4 clinical net drug-drug interaction based on CYP3A4 inhibition, inactivation, and induction determined in vitro. *Drug Metab Dispos* **36**:1698-1708.
- Fujino H, Shimada S, Yamada I, Hirano M, Tsunenari Y, and Kojima J (2003) Studies on the interaction between fibrates and statins using human hepatic microsomes. *Arzneimittelforschung* **53**:701-707.
- Giacomini KM, Huang SM, Tweedie DJ, Benet LZ, Brouwer KL, Chu X, Dahlin A, Evers R, Fischer V, Hillgren KM, Hoffmaster KA, Ishikawa T, Keppler D, Kim RB, Lee CA, Niemi M, Polli JW, Sugiyama Y, Swaan PW, Ware JA, Wright SH, Yee SW, Zamek-Gliszczyński MJ, and Zhang L (2010) Membrane transporters in drug development. *Nat Rev Drug Discov* **9**:215-236.



- Glaeser H, Drescher S, Eichelbaum M, and Fromm MF (2005) Influence of rifampicin on the expression and function of human intestinal cytochrome P450 enzymes. *Br J Clin Pharmacol* **59**:199-206.
- Hatorp V, Hansen KT, and Thomsen MS (2003) Influence of drugs interacting with CYP3A4 on the pharmacokinetics, pharmacodynamics, and safety of the prandial glucose regulator repaglinide. *J Clin Pharmacol* **43**:649-660.
- Hatorp V, Oliver S, and Su CA (1998) Bioavailability of repaglinide, a novel antidiabetic agent, administered orally in tablet or solution form or intravenously in healthy male volunteers. *Int J Clin Pharmacol Ther* **36**:636-641.
- Honkalammi J, Niemi M, Neuvonen PJ, and Backman JT (2011a) Dose-dependent interaction between gemfibrozil and repaglinide in humans: strong inhibition of CYP2C8 with subtherapeutic gemfibrozil doses. *Drug Metab Dispos* **39**:1977-1986.
- Honkalammi J, Niemi M, Neuvonen PJ, and Backman JT (2011b) Mechanism-based inactivation of CYP2C8 by gemfibrozil occurs rapidly in humans. *Clin Pharmacol Ther* **89**:579-586.
- Honkalammi J, Niemi M, Neuvonen PJ, and Backman JT (2012) Gemfibrozil is a strong inactivator of CYP2C8 in very small multiple doses. *Clin Pharmacol Ther* **91**:846-855.
- Huang SM and Rowland M (2012) The role of physiologically based pharmacokinetic modeling in regulatory review. *Clin Pharmacol Ther* **91**:542-549.
- Jones HM, Barton HA, Lai Y, Bi YA, Kimoto E, Kempshall S, Tate SC, El-Kattan A, Houston JB, Galetin A, and Fenner KS (2012) Mechanistic pharmacokinetic modeling for the prediction of transporter-mediated disposition in humans from sandwich culture human hepatocyte data. *Drug Metab Dispos* **40**:1007-1017.
- Kajosaari LI, Laitila J, Neuvonen PJ, and Backman JT (2005a) Metabolism of repaglinide by CYP2C8 and CYP3A4 in vitro: effect of fibrates and rifampicin. *Basic Clin Pharmacol Toxicol* **97**:249-256.
- Kajosaari LI, Niemi M, Neuvonen M, Laitila J, Neuvonen PJ, and Backman JT (2005b) Cyclosporine markedly raises the plasma concentrations of repaglinide. *Clin Pharmacol Ther* **78**:388-399.
- Kato M, Chiba K, Hisaka A, Ishigami M, Kayama M, Mizuno N, Nagata Y, Takakuwa S, Tsukamoto Y, Ueda K, Kusahara H, Ito K, and Sugiyama Y (2003) The intestinal first-pass metabolism of substrates of CYP3A4 and P-glycoprotein-quantitative analysis based on information from the literature. *Drug Metab Pharmacokinet* **18**:365-372.

- Kimoto E, Yoshida K, Balogh LM, Bi YA, Maeda K, El-Kattan A, Sugiyama Y, and Lai Y (2012) Characterization of Organic Anion Transporting Polypeptide (OATP) Expression and Its Functional Contribution to the Uptake of Substrates in Human Hepatocytes. *Mol Pharm*.
- Korzekwa KR, Nagar S, Tucker J, Weiskircher EA, Bhoopathy S, and Hidalgo IJ (2012) Models to predict unbound intracellular drug concentrations in the presence of transporters. *Drug Metab Dispos* **40**:865-876.
- Lapple F, von Richter O, Fromm MF, Richter T, Thon KP, Wisser H, Griese EU, Eichelbaum M, and Kivisto KT (2003) Differential expression and function of CYP2C isoforms in human intestine and liver. *Pharmacogenetics* **13**:565-575.
- Lau YY, Huang Y, Frassetto L, and Benet LZ (2007) Effect of OATP1B transporter inhibition on the pharmacokinetics of atorvastatin in healthy volunteers. *Clin Pharmacol Ther* **81**:194-204.
- Liu L and Pang KS (2005) The roles of transporters and enzymes in hepatic drug processing. *Drug Metab Dispos* **33**:1-9.
- Luo G, Cunningham M, Kim S, Burn T, Lin J, Sinz M, Hamilton G, Rizzo C, Jolley S, Gilbert D, Downey A, Mudra D, Graham R, Carroll K, Xie J, Madan A, Parkinson A, Christ D, Selling B, LeCluyse E, and Gan LS (2002) CYP3A4 induction by drugs: correlation between a pregnane X receptor reporter gene assay and CYP3A4 expression in human hepatocytes. *Drug Metab Dispos* **30**:795-804.
- Maeda K, Ikeda Y, Fujita T, Yoshida K, Azuma Y, Haruyama Y, Yamane N, Kumagai Y, and Sugiyama Y (2011) Identification of the rate-determining process in the hepatic clearance of atorvastatin in a clinical cassette microdosing study. *Clin Pharmacol Ther* **90**:575-581.
- Mandic Z and Gabelica V (2006) Ionization, lipophilicity and solubility properties of repaglinide. *Journal of pharmaceutical and biomedical analysis* **41**:866-871.
- Menoche K, Kenworthy KE, Houston JB, and Galetin A (2012) Use of mechanistic modeling to assess interindividual variability and interspecies differences in active uptake in human and rat hepatocytes. *Drug Metab Dispos* **40**:1744-1756.
- Niemi M, Backman JT, Fromm MF, Neuvonen PJ, and Kivisto KT (2003a) Pharmacokinetic interactions with rifampicin : clinical relevance. *Clin Pharmacokinet* **42**:819-850.
- Niemi M, Backman JT, Kajosaari LI, Leathart JB, Neuvonen M, Daly AK, Eichelbaum M, Kivisto KT, and Neuvonen PJ (2005) Polymorphic organic anion transporting polypeptide 1B1 is a major determinant of repaglinide pharmacokinetics. *Clin Pharmacol Ther* **77**:468-478.

- Niemi M, Backman JT, Neuvonen M, and Neuvonen PJ (2003b) Effects of gemfibrozil, itraconazole, and their combination on the pharmacokinetics and pharmacodynamics of repaglinide: potentially hazardous interaction between gemfibrozil and repaglinide. *Diabetologia* **46**:347-351.
- Niemi M, Backman JT, Neuvonen M, Neuvonen PJ, and Kivisto KT (2000) Rifampin decreases the plasma concentrations and effects of repaglinide. *Clin Pharmacol Ther* **68**:495-500.
- Niemi M, Leathart JB, Neuvonen M, Backman JT, Daly AK, and Neuvonen PJ (2003c) Polymorphism in CYP2C8 is associated with reduced plasma concentrations of repaglinide. *Clin Pharmacol Ther* **74**:380-387.
- Obach RS, Walsky RL, Venkatakrishnan K, Gaman EA, Houston JB, and Tremaine LM (2006) The utility of in vitro cytochrome P450 inhibition data in the prediction of drug-drug interactions. *J Pharmacol Exp Ther* **316**:336-348.
- Paine MF, Hart HL, Ludington SS, Haining RL, Rettie AE, and Zeldin DC (2006) The human intestinal cytochrome P450 "pie". *Drug Metab Dispos* **34**:880-886.
- Pang KS and Rowland M (1977) Hepatic clearance of drugs. II. Experimental evidence for acceptance of the "well-stirred" model over the "parallel tube" model using lidocaine in the perfused rat liver in situ preparation. *J Pharmacokinetic Biopharm* **5**:655-680.
- Plum A, Muller LK, and Jansen JA (2000) The effects of selected drugs on the in vitro protein binding of repaglinide in human plasma. *Methods Find Exp Clin Pharmacol* **22**:139-143.
- Reitman ML, Chu X, Cai X, Yabut J, Venkatasubramanian R, Zajic S, Stone JA, Ding Y, Witter R, Gibson C, Roupe K, Evers R, Wagner JA, and Stoch A (2011) Rifampin's acute inhibitory and chronic inductive drug interactions: experimental and model-based approaches to drug-drug interaction trial design. *Clin Pharmacol Ther* **89**:234-242.
- Rodgers T and Rowland M (2006) Physiologically based pharmacokinetic modelling 2: predicting the tissue distribution of acids, very weak bases, neutrals and zwitterions. *J Pharm Sci* **95**:1238-1257.
- Rostami-Hodjegan A (2012) Physiologically based pharmacokinetics joined with in vitro-in vivo extrapolation of ADME: a marriage under the arch of systems pharmacology. *Clin Pharmacol Ther* **92**:50-61.
- Rowland M, Peck C, and Tucker G (2011) Physiologically-based pharmacokinetics in drug development and regulatory science. *Annu Rev Pharmacol Toxicol* **51**:45-73.

- Sall C, Houston JB, and Galetin A (2012) A comprehensive assessment of repaglinide metabolic pathways: impact of choice of in vitro system and relative enzyme contribution to in vitro clearance. *Drug Metab Dispos* **40**:1279-1289.
- Scott LJ (2012) Repaglinide: a review of its use in type 2 diabetes mellitus. *Drugs* **72**:249-272.
- Shitara Y, Hirano M, Sato H, and Sugiyama Y (2004) Gemfibrozil and its glucuronide inhibit the organic anion transporting polypeptide 2 (OATP2/OATP1B1:SLC21A6)-mediated hepatic uptake and CYP2C8-mediated metabolism of cerivastatin: analysis of the mechanism of the clinically relevant drug-drug interaction between cerivastatin and gemfibrozil. *J Pharmacol Exp Ther* **311**:228-236.
- Shitara Y, Horie T, and Sugiyama Y (2006) Transporters as a determinant of drug clearance and tissue distribution. *Eur J Pharm Sci* **27**:425-446.
- Shitara Y and Sugiyama Y (2006) Pharmacokinetic and pharmacodynamic alterations of 3-hydroxy-3-methylglutaryl coenzyme A (HMG-CoA) reductase inhibitors: drug-drug interactions and interindividual differences in transporter and metabolic enzyme functions. *Pharmacol Ther* **112**:71-105.
- Skerjanec A, Wang J, Maren K, and Rojkaer L (2010) Investigation of the pharmacokinetic interactions of deferasirox, a once-daily oral iron chelator, with midazolam, rifampin, and repaglinide in healthy volunteers. *J Clin Pharmacol* **50**:205-213.
- Tornio A, Niemi M, Neuvonen M, Laitila J, Kalliokoski A, Neuvonen PJ, and Backman JT (2008) The effect of gemfibrozil on repaglinide pharmacokinetics persists for at least 12 h after the dose: evidence for mechanism-based inhibition of CYP2C8 in vivo. *Clin Pharmacol Ther* **84**:403-411.
- Tornio A, Niemi M, Neuvonen PJ, and Backman JT (2012) Drug interactions with oral antidiabetic agents: pharmacokinetic mechanisms and clinical implications. *Trends Pharmacol Sci* **33**:312-322.
- USFDA (2012) Drug interaction studies - study design, data analysis, implications for dosing, and labeling recommendations. *Center for Drug Evaluation and Research (CDER)*.
- Varma MV, Gardner I, Steyn SJ, Nkansah P, Rotter CJ, Whitney-Pickett C, Zhang H, Di L, Cram M, Fenner KS, and El-Kattan AF (2012a) pH-Dependent solubility and permeability criteria for provisional biopharmaceutics classification (BCS and BDDCS) in early drug discovery. *Mol Pharm* **9**:1199-1212.
- Varma MV, Lai Y, Feng B, Litchfield J, Goosen TC, and Bergman A (2012b) Physiologically based modeling of pravastatin transporter-mediated hepatobiliary disposition and drug-drug interactions. *Pharm Res* **29**:2860-2873.

- Varma MV, Lai Y, Kimoto E, Goosen TC, El-Kattan AF, and Kumar V (2013) Mechanistic modeling to predict the transporter- and enzyme-mediated drug-drug interactions of repaglinide. *Pharm Res* (**in press**).
- Varma MV, Obach RS, Rotter C, Miller HR, Chang G, Steyn SJ, El-Kattan A, and Troutman MD (2010) Physicochemical space for optimum oral bioavailability: contribution of human intestinal absorption and first-pass elimination. *J Med Chem* **53**:1098-1108.
- Varma MV, Sateesh K, and Panchagnula R (2005) Functional role of P-glycoprotein in limiting intestinal absorption of drugs: contribution of passive permeability to P-glycoprotein mediated efflux transport. *Mol Pharm* **2**:12-21.
- Watanabe T, Kusuhara H, Maeda K, Shitara Y, and Sugiyama Y (2009) Physiologically based pharmacokinetic modeling to predict transporter-mediated clearance and distribution of pravastatin in humans. *J Pharmacol Exp Ther* **328**:652-662.
- Westphal K, Weinbrenner A, Zschiesche M, Franke G, Knoke M, Oertel R, Fritz P, von Richter O, Warzok R, Hachenberg T, Kauffmann HM, Schrenk D, Terhaag B, Kroemer HK, and Siegmund W (2000) Induction of P-glycoprotein by rifampin increases intestinal secretion of talinolol in human beings: a new type of drug/drug interaction. *Clin Pharmacol Ther* **68**:345-355.
- Wu CY and Benet LZ (2005) Predicting drug disposition via application of BCS: transport/absorption/ elimination interplay and development of a biopharmaceutics drug disposition classification system. *Pharm Res* **22**:11-23.
- Zheng HX, Huang Y, Frassetto LA, and Benet LZ (2009) Elucidating rifampin's inducing and inhibiting effects on glyburide pharmacokinetics and blood glucose in healthy volunteers: unmasking the differential effects of enzyme induction and transporter inhibition for a drug and its primary metabolite. *Clin Pharmacol Ther* **85**:78-85.

DMD #50583

## FOOTNOTES

All authors are full-time employees of Pfizer Inc. The authors have no conflicts of interest that are directly relevant to this study.

Figure Captions:

**Figure 1.** PBPK model predictions of repaglinide pharmacokinetics and drug-drug interactions with rifampicin. A. Observed and simulated mean plasma concentration-time profiles of repaglinide following single 2 mg intravenous infusion (circles and dashed line) and 0.5 mg oral dose (squares and solid line) (Hatorp et al., 1998; Skerjanec et al., 2010). B. Mean plasma concentration-time profiles of single 0.5 mg oral repaglinide dosed 12.5h after the last dose of once-daily 600 mg rifampicin is shown. Open (solid line) and closed (dotted line) data points represent mean observed (simulated) values in the control and rifampicin treatment groups, respectively (Niemi et al., 2000). Grey lines represent plasma concentration-time profiles in individual trials (5 trials x 10 subjects).

**Figure 2.** A. Dynamic and static model predicted AUCRs of repaglinide dosed at different time after the last dose of rifampicin. B. Observed versus predicted AUCRs. Observed mean AUCRs were taken from separate clinical studies (Niemi et al., 2000; Hatorp et al., 2003; Bidstrup et al., 2004). For dynamic model simulations, dosage regimen of repaglinide and rifampicin is similar to the original reported study design: \*5-day rifampicin treatment for these data points – all other points involves 7-day rifampicin treatment. Error bars represent range or 90% confidence interval of the observed AUCRs. Dashed lines represent  $\pm 25\%$  deviation from unity (solid line).

DMD #50583

**Figure 3.** Effect of hepatic fraction metabolism ( $f_{m_{CYP3A4}}$ ) on the static model-based predictions of AUCRs of repaglinide dosed at different time after the last dose of rifampicin.

**Figure 4.** Simulated contribution of individual components of CYP3A4 induction, OATP1B1 inhibition and CYPs inhibition to the net-effect of the predicted repaglinide-rifampicin DDIs by (A) dynamic or (B) static models. Data points represent observed mean AUC ratios.

**Figure 5.** Effect of rifampicin treatment on the intrinsic metabolic and transport clearances of repaglinide. PBPK model simulations of the effect of rifampicin treatment on the (A) change in CYP3A4 metabolic activity in the intestine and liver, (B) fraction of repaglinide dose metabolized in intestine and liver, and (C) change in OATP1B1 activity. Arrows indicate time of single repaglinide dose following rifampicin treatment.



**Table 1** Summary of input parameters for repaglinide dynamic and static mechanistic models.

Parameters	Repaglinide	Source	Rifampicin <sup>†</sup>	Source
<b>Physicochemical properties</b>				
Molecular weight (g/mol)	452.6	ACD	823	
log P	4.87	ACD	3.28	
Compound type	Ampholyte	ACD	Ampholyte	
pK <sub>a</sub>	4.19 & 5.78	ACD	1.7 & 7.9	
Fraction unbound (f <sub>u,p</sub> )	0.015	(Plum et al., 2000)	0.15	
Blood/plasma ratio (Rb)	0.62	(Kajosaari et al., 2005a)	0.90	
<b>Absorption</b>				
Absorption type	ADAM		First-order	
Fraction absorbed	>0.95	(Hatorp et al., 1998; Varma et al., 2010)	1.0	
Caco-2 permeability (×10 <sup>-6</sup> cm/s)	26.1	In-house data		
Absorption Scalar	1.873	In-house data		
K <sub>a</sub>			0.51	
f <sub>u,gut</sub>	1	Assumed	0.15	
<b>Distribution</b>				
Distribution model	Whole-body PBPK	(Rodgers et al.)(Rodgers and Rowland, 2006)	Minimal PBPK	
<b>Elimination</b>				
Intravenous clearance (L/h)	32.6	(Hatorp et al., 1998)	7.0	
<i>In vivo</i> CL <sub>int,h</sub> (mL/min/kg)	1326 <sup>e</sup>	(Hatorp et al., 1998)		
CL <sub>int,CYP2C8</sub> (μL/min/mg-microsomal protein)	93 <sup>v</sup>	(Kajosaari et al., 2005a)		
CL <sub>int,CYP3A4</sub> (μL/min/mg-microsomal protein)	38 <sup>v</sup>	(Kajosaari et al., 2005a)		
Renal elimination (%)	<1%	(Hatorp et al., 1998)		
<b>Hepatobiliary transport</b>				
Liver unbound fraction (Intra-/extra-cellular)	0.143/0.028	Calculated		
PS <sub>pd</sub> (μL/min/10 <sup>-6</sup> cells)	24	SCHH data (Varma et al., 2013)		
PS <sub>influx,active</sub> (μL/min/10 <sup>-6</sup> cells)	37	SCHH data (Varma et al., 2013)		
Scaling factor (Active) for Dynamic model	16.9	Estimated* (Varma et al., 2013)		
Scaling factor (Active) for Static model	19.5	Estimated*		
CL <sub>int,bile</sub> (μL/min/10 <sup>-6</sup> cells)	0	SCHH data (Varma et al., 2013)		
<b>Rifampicin Interaction potency</b>				
CYP3A4 E <sub>max</sub>			49.5	In-house data
CYP3A4 EC <sub>50</sub> (μM)			0.228	In-house data
CYP3A4 K <sub>i</sub> (μM)			18.5	(Kajosaari et al., 2005a)
CYP2C8 K <sub>i</sub> (μM)			30.2	(Kajosaari et al., 2005a)
OATP1B1 K <sub>i</sub> (μM)			0.93	(Varma et al., 2012b)

DMD #50583

\*Estimated by fitting to intravenous pharmacokinetics data (PBPK model) or *in vivo*  $CL_{int,h}$  (Static model).  
See Methods.

<sup>∞</sup>  $CL_{int,h}$  from intravenous hepatic blood clearance ( $CL_h$ ) was calculated using  $CL_{int,h} = CL_h / (f_{u,b} \times (1 - CL_h/Q_h))$ .

<sup>v</sup> *In vitro*  $f_{mCYP3A4}$  equaling to 0.29.

<sup>†</sup> Input parameters were directly adopted from compound files of Simcyp compound library.  
ACD, Calculated using Advanced Chemistry Development (ACD/Labs) Software V11.02. (SciFinder 2007.1)

ADAM, Advanced dissolution, absorption and metabolism model; P, partition coefficient;  $pK_a$ , acid dissociation constant.

Table 2. Summary of the dynamic and the static mechanistic model based predictions of repaglinide-rifampicin interactions.

Dosage regimen*	Observed AUCR	PBPK model prediction			Static model prediction					
		$CL_{int,h}/CL'_{int,h}$	$Fg'/Fg$	AUCR	$[I_{u,max,in}]$ ( $\mu M$ ) <sup>∞</sup>	$[I_{u,gut}]$ ( $\mu M$ ) <sup>∞</sup>	R-value <sup>‡</sup>	$CL_{int,h}/CL'_{int,h}$	$Fg'/Fg$	AUCR
0h	0.52 (Bidstrup et al., 2004)	1.70	0.40	0.68	1.76	3.75	3.1	1.95	0.30	0.59
1h	0.69 (Hatorp et al., 2003)	1.83	0.41	0.75	1.76	3.75	3.1	1.95	0.30	0.59
12.5h	0.43 (Niemi et al., 2000)	1.15	0.33	0.38	0.27	0	1.3	0.91	0.26	0.24
24h	0.20 (Bidstrup et al., 2004)	0.88	0.33	0.29	0.02	0	1.0	0.73	0.26	0.19
APPE				24%						19%
RMSE				0.10						0.11
AFE				1.24						1.26

\*Time of repaglinide oral dose after the last dose of rifampicin.

<sup>∞</sup>For static model, CYP3A4 induction was assumed constant for 24h after the rifampicin treatment, and was calculated using 1.76 $\mu M$  for  $[I_{u,max,in}]$  or 3.75 $\mu M$  for  $[I_{u,gut}]$ .

<sup>‡</sup>R-value for OATP1B1-mediated interaction (Giacomini et al., 2010; USFDA, 2012) was calculated:  $1+(I_{u,max,in}/K_i)$ .

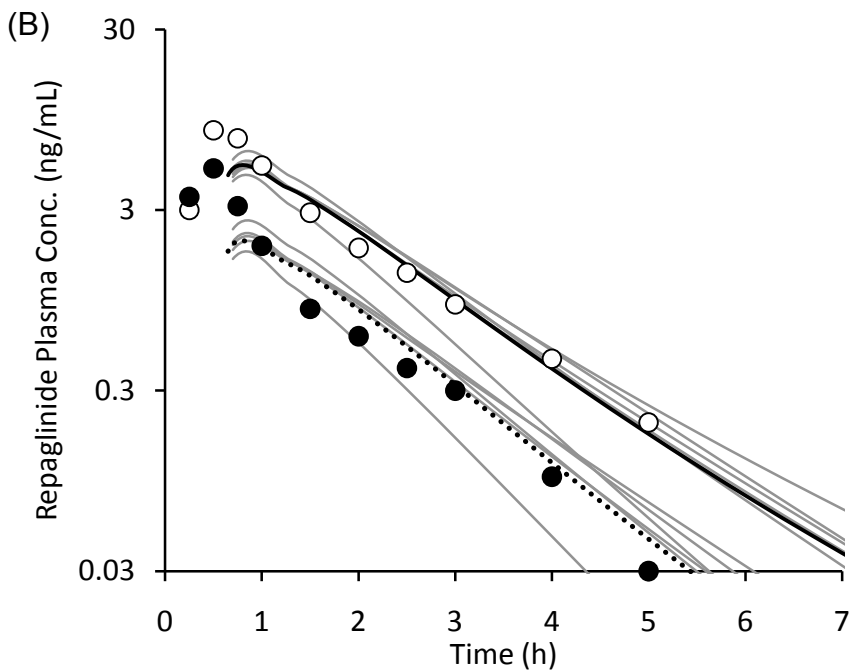
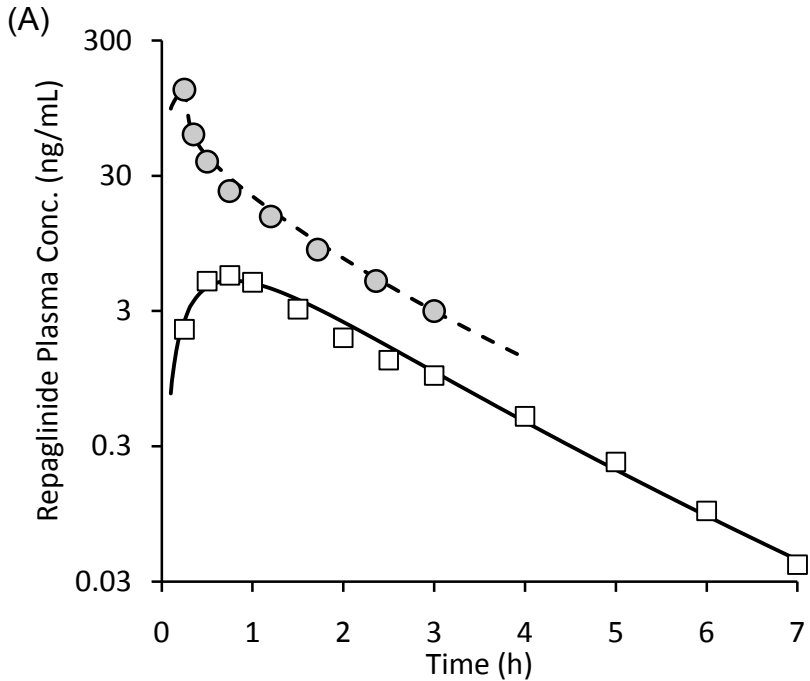


Figure 1

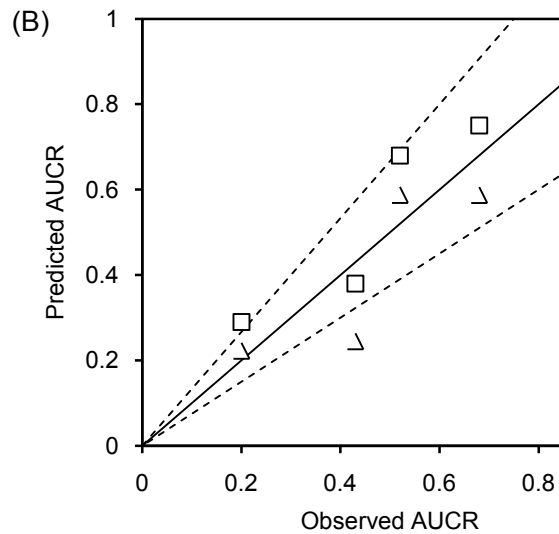
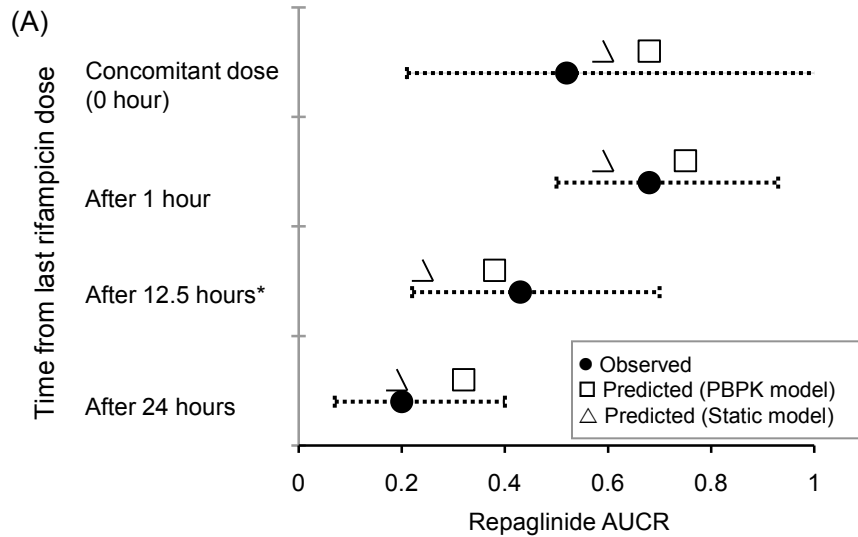


Figure 2

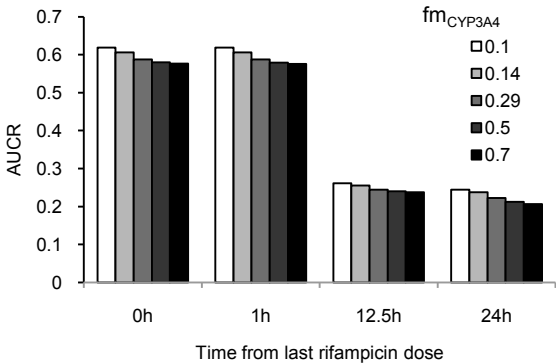


Figure 3

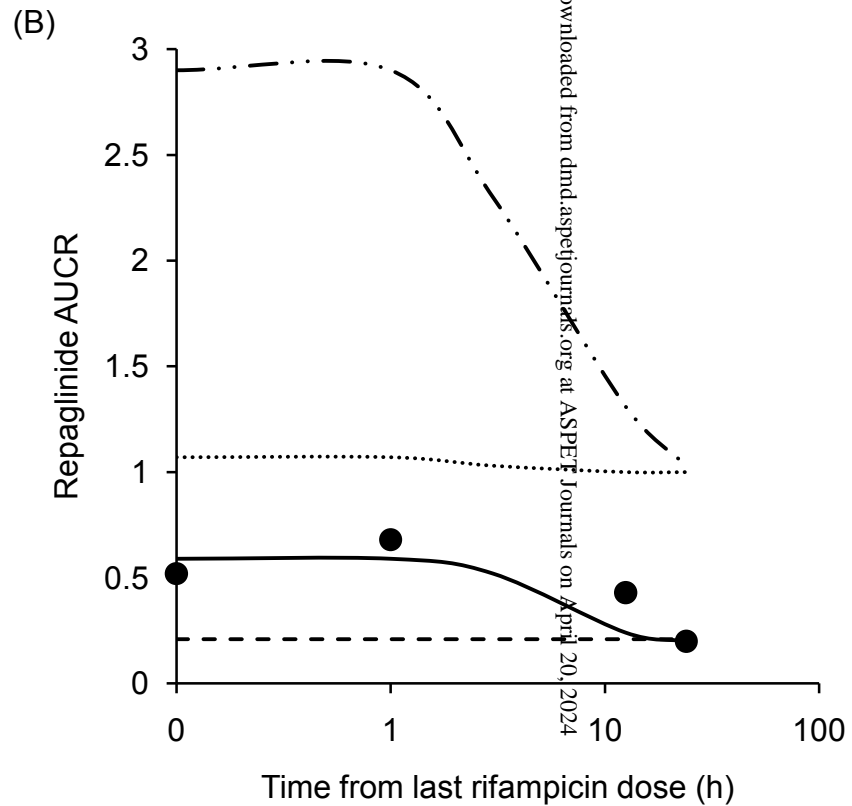
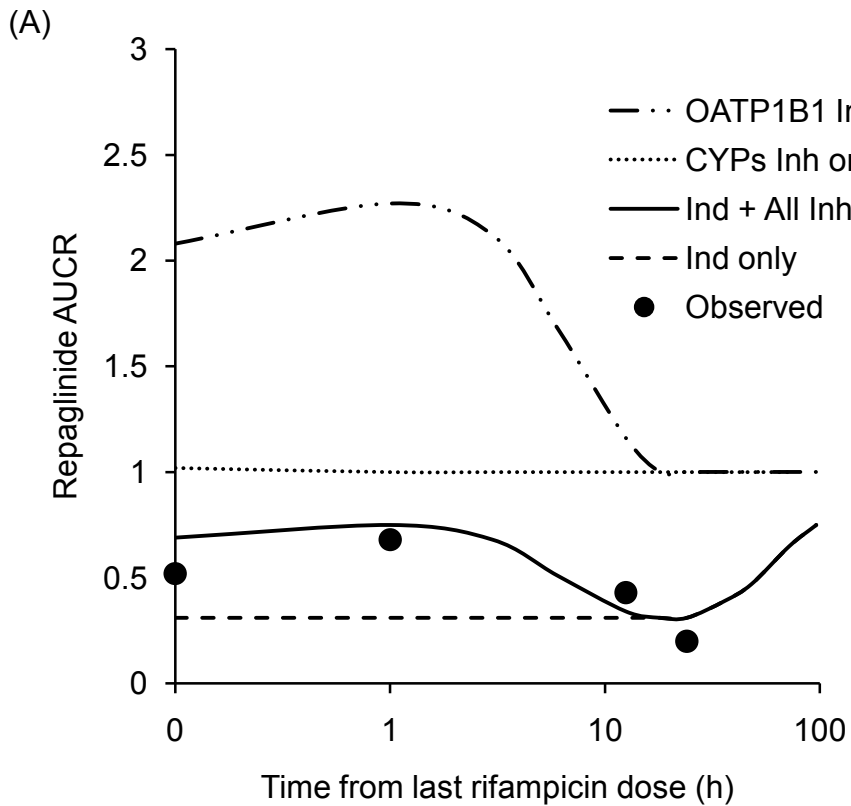


Figure 4

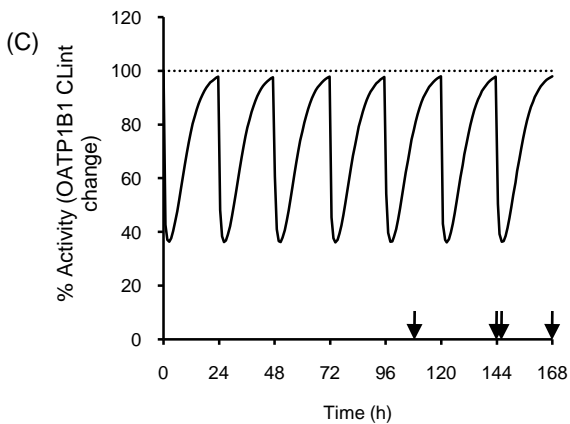
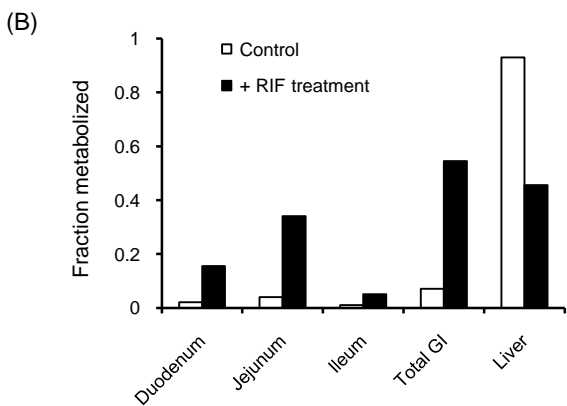
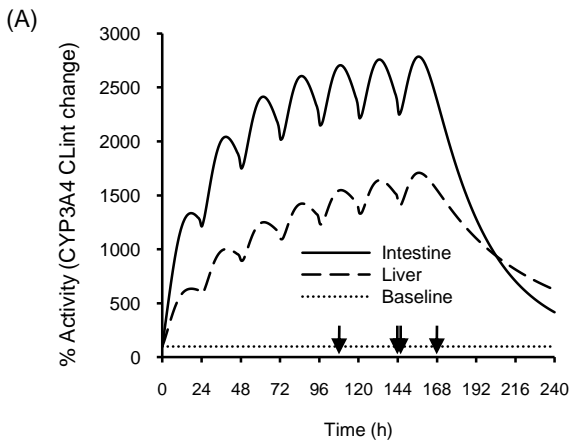


Figure 5